

## Supplementary Information

### Thermal Control of Photothermal Implants Inspired by Polar Bear Skin for the Treatment of Infected Bone Defects

Mingyue Han<sup>a‡</sup>, Xinlong Li<sup>b‡</sup>, Shijie Shi<sup>a</sup>, Ailin Hou<sup>a</sup>, Han Yin<sup>a</sup>, Lizhong Sun<sup>a</sup>, Jianshu Li<sup>b</sup>, Jun Luo<sup>b</sup>, Jiyao Li<sup>a\*</sup>, Jiaojiao Yang<sup>a\*</sup>

#### Affiliations:

a State Key Laboratory of Oral Diseases, National Clinical Research Center for Oral Diseases, Department of Cariology and Endodontics, West China Hospital of Stomatology, Sichuan University, Chengdu 610041, China

b College of Polymer Science and Engineering, Sichuan University, Chengdu 610065, China

‡The authors contribute equally to this work.

\*: Correspondence author

Correspondence to: Jiaojiao Yang, email: [jiaojiao.yang@scu.edu.cn](mailto:jiaojiao.yang@scu.edu.cn); Jiyao Li, email: [jiyaoliscu@163.com](mailto:jiyaoliscu@163.com)

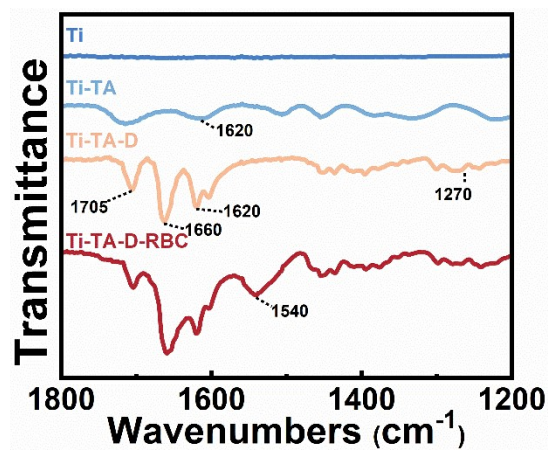


**Fig. S1** ATR-FTIR spectra displaying the range from 1800  $\text{cm}^{-1}$  and 1200  $\text{cm}^{-1}$ .

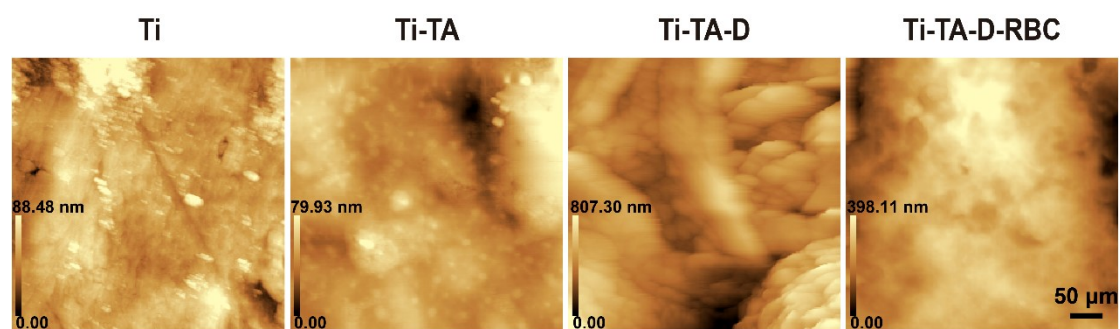


**Fig. S2** Representative AFM images of the considered samples.

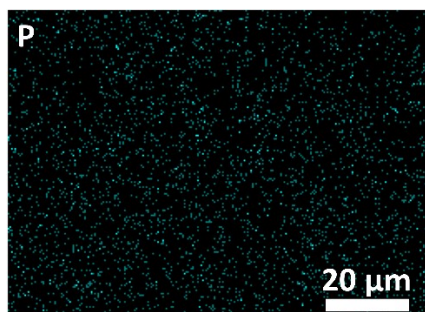


**Fig. S3** Elemental mapping of phosphorous (P) on Ti-TA-D-RBC.

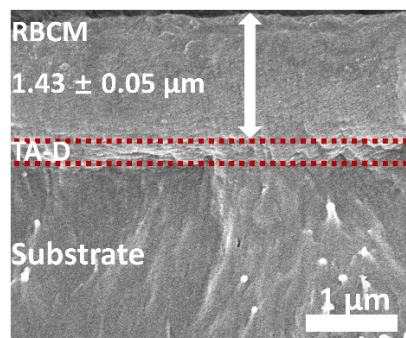


**Fig. S4** Average thickness of RBC membrane coating.

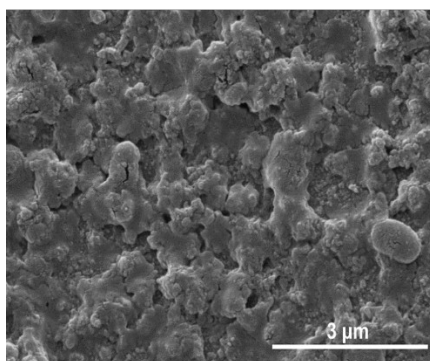


**Fig. S5** The refrigerated scanning electron microscope (RSEM) image of Ti-TA-D-RBC.

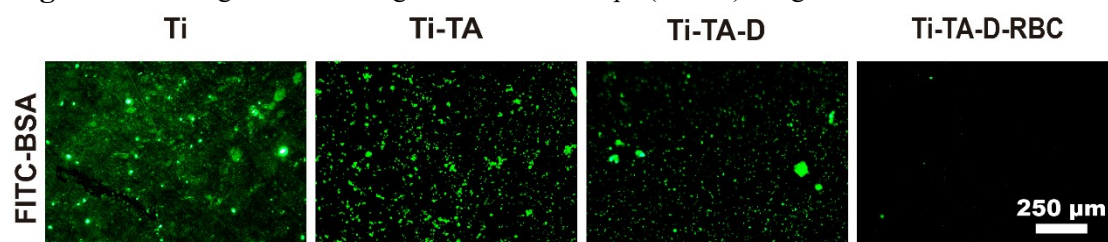


**Fig. S6** Fluorescence images of FITC-BSA adhered to the surface.

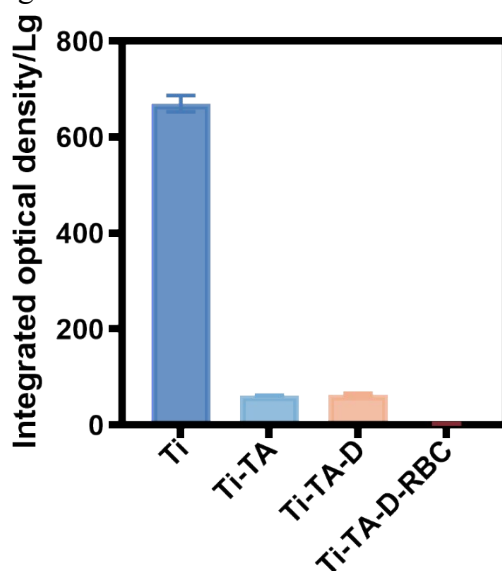


**Fig. S7** The corresponding integrated optical density (IOD) values derived from fluorescence images of FITC-BSA adhered to the surface.

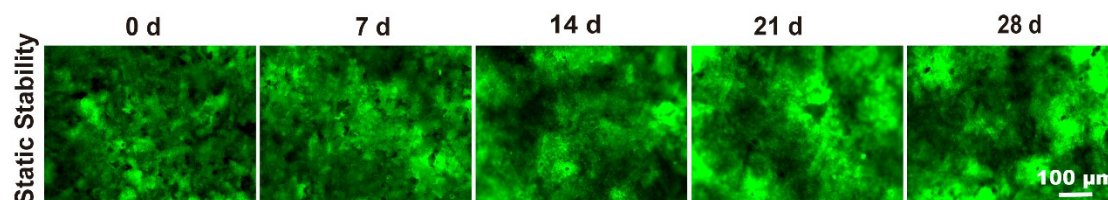


**Fig. S8** Fluorescence images of Ti-TA-D-RBC to assess its static stability at 0 d, 7 d, 14 d, 21 d, and 28 d.

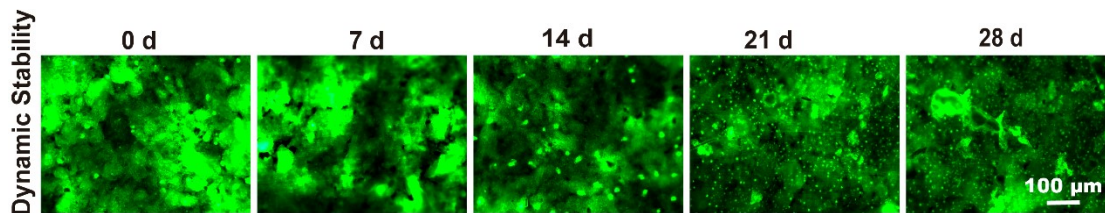


**Fig. S9** Fluorescence images of Ti-TA-D-RBC to assess dynamic stability.

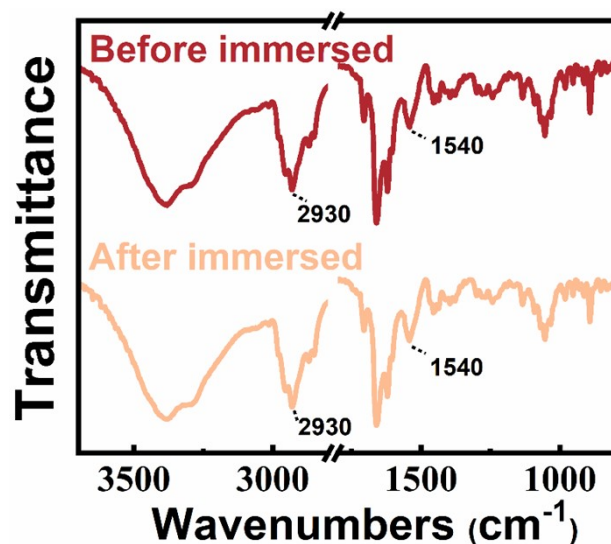


**Fig. S10** ATR-FTIR spectra of Ti-TA-D-RBC before/after immersed in PBS for 7 d to assess its static stability.

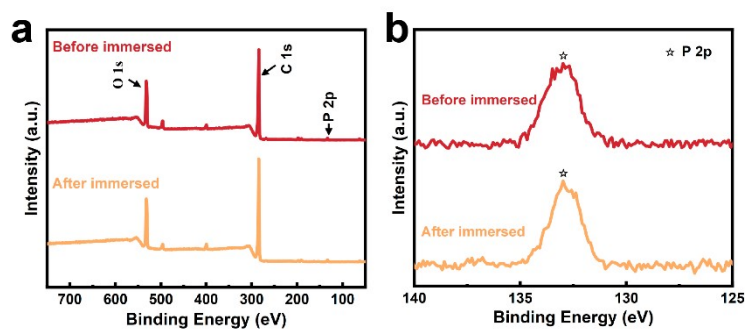


**Fig. S11** XPS spectra of Ti-TA-D-RBC before/after immersed in PBS for 7 d to assess its static stability. (a) XPS survey spectra; (b) High-resolution XPS spectra range from 140 to 125 eV to magnify P 2p.

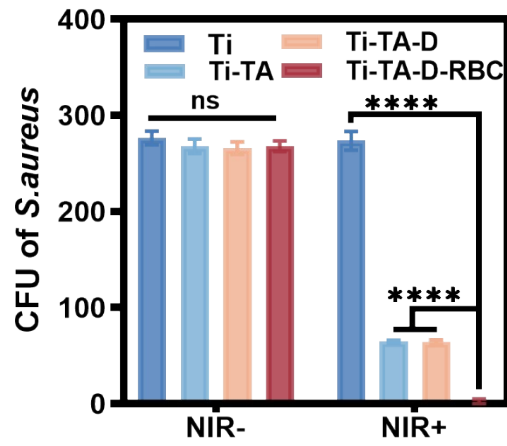


**Fig. S12** Counts of *S. aureus* colonies treated with each group.

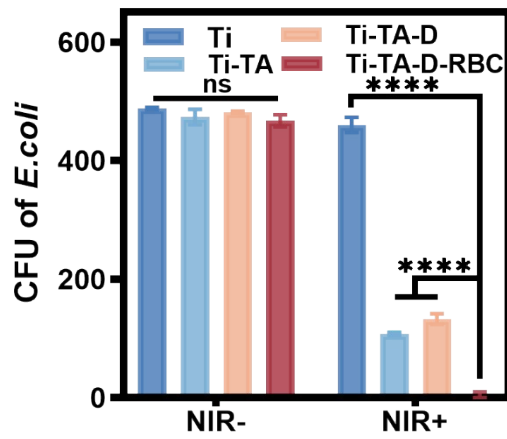


**Fig. S13** Counts of *E. coli* colonies treated with each group.

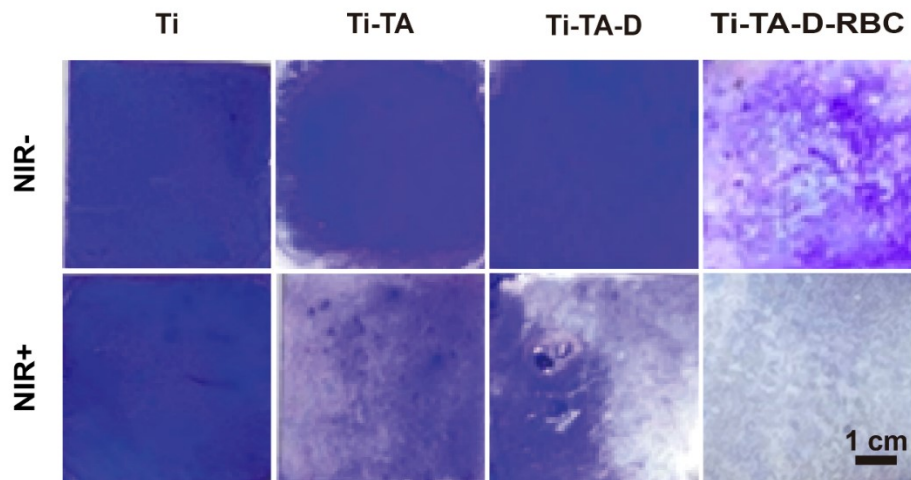


**Fig. S14** Representative images of biofilms, visualized through staining with crystal violet staining.

**Table S1** The comparison of Ti-TA/Ti-TA-D and Ti-TA-D-RBC under NIR irradiation *in vitro*.

group	Temperature under NIR for 10 min	Anti-bacterial ratio of <i>S.aureus</i>	Anti-bacterial ratio of <i>E.coli</i>	Anti-biofilm ratio
Ti-TA/Ti-TA-D	48.5 ± 2.9°C /	76.63 ± 0.55% /	77.94 ± 0.52% /	25.33 ± 0.64% /
	43.23 ± 2.06°C	76.87 ± 0.96%	72.81 ± 1.79%	20.02 ± 0.58%
Ti-TA-D-RBC	63.2 ± 1.3°C	99.24 ± 0.91%	98.96 ± 1.02%	95.19 ± 1.06%
Increasing ratio	1.30 / 1.46 times	1.30 times	1.27 times	1.80 times

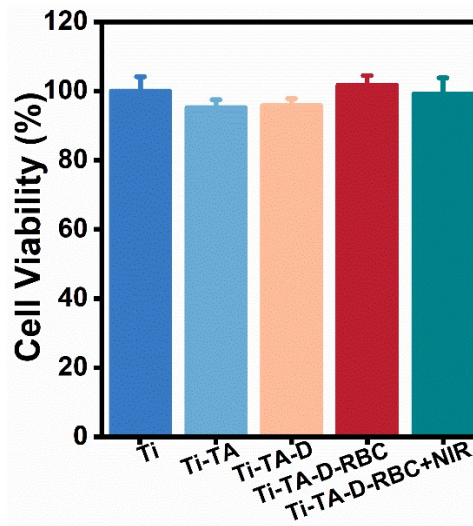


**Fig. S15** The cell viability of BMSCs incubated with each group tested via cell counting Kit-8 (CCK-8) for 24 h (mean ± standard deviation, n = 6).

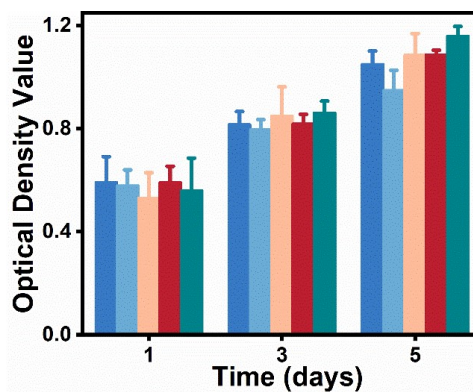


**Fig. S16** Cell proliferation of BMSCs measured by CCK-8 for 1 d, 3 d, and 5 d.

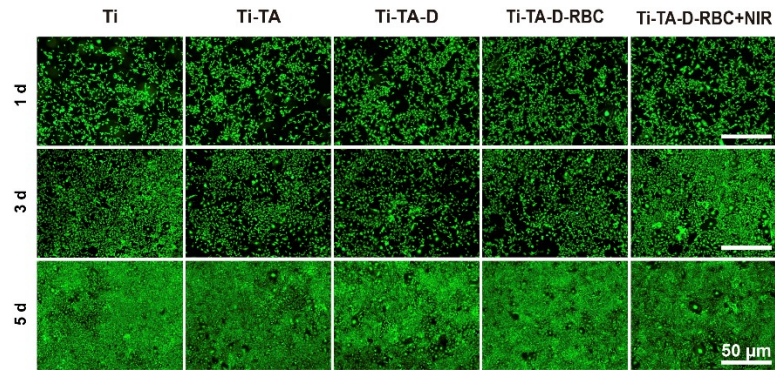


**Fig. S17** Live/Dead cell staining images of BMSCs cultured on the indicated surfaces for 1 d, 3 d, and 5 d.

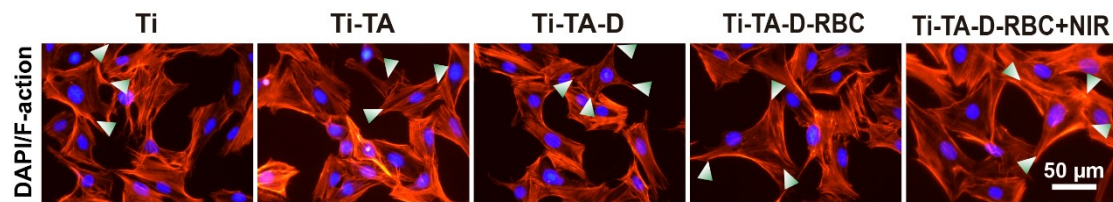


**Fig. S18** Cell morphologies of BMSCs cultured with each group for 3 days.

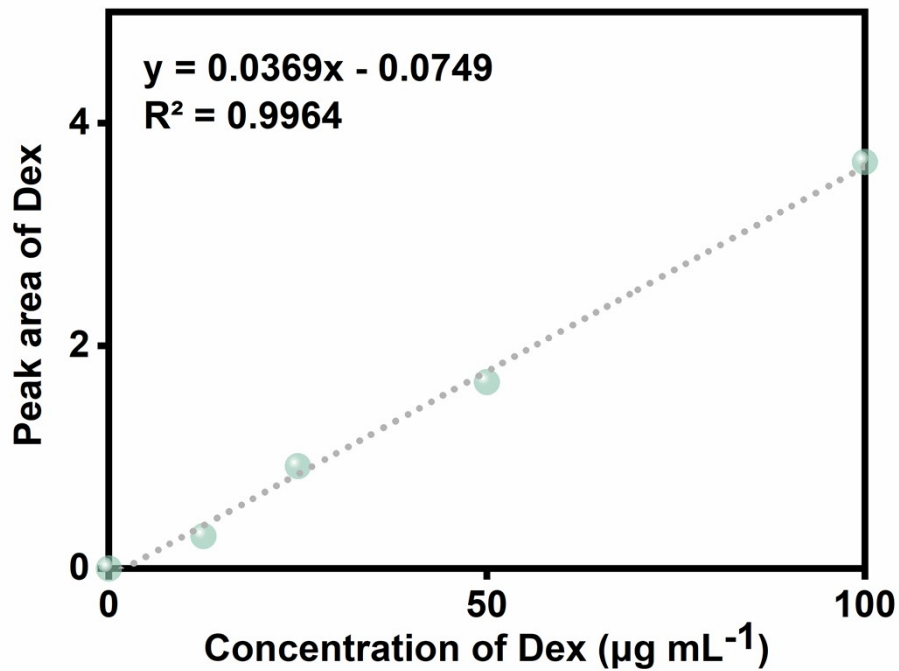


**Fig. S19** Linear relationship between concentration and peak area of Dex standard solution.

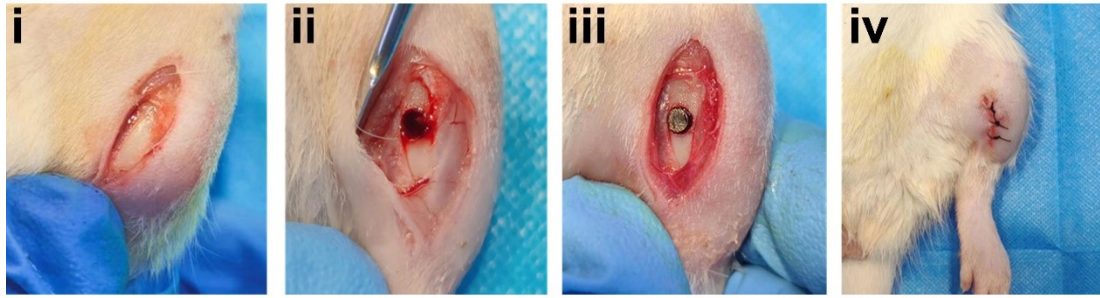


**Fig. S20** Representative photos of our surgical procedure.

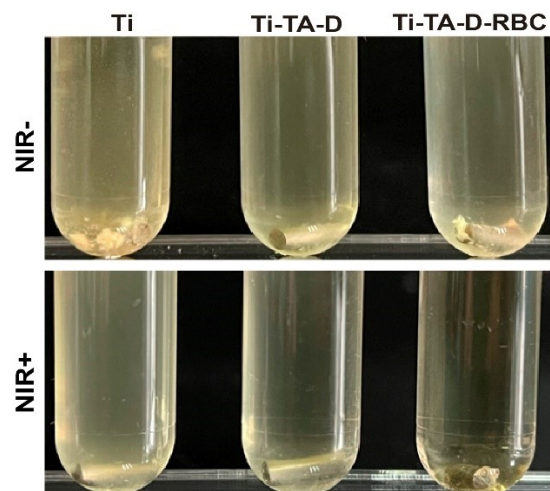


**Fig. S21** Photos of LB cultured with the implants.

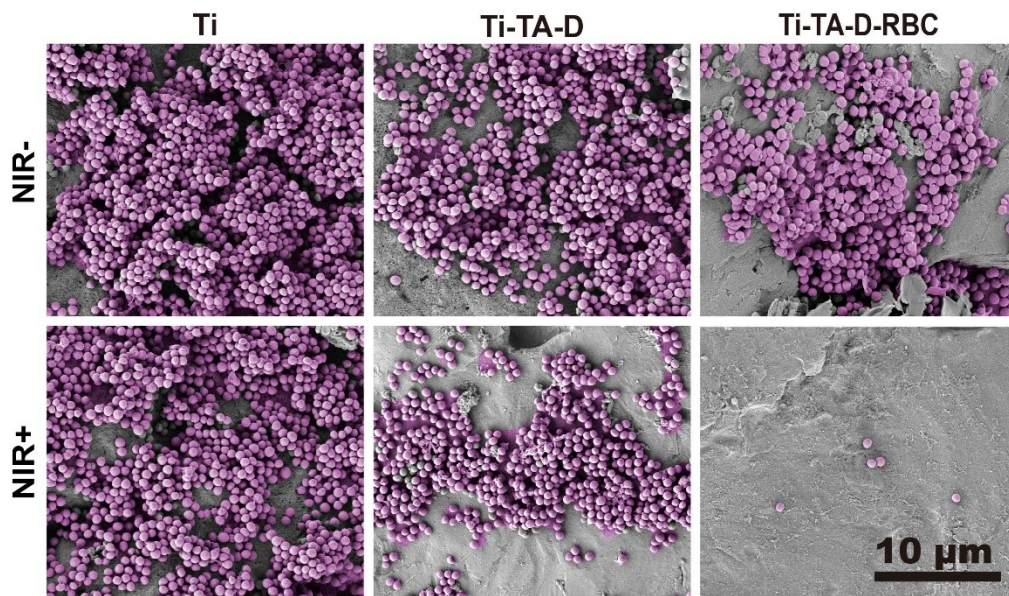


**Fig. S22** SEM images of the implant's surface one week post-implantation of each group.

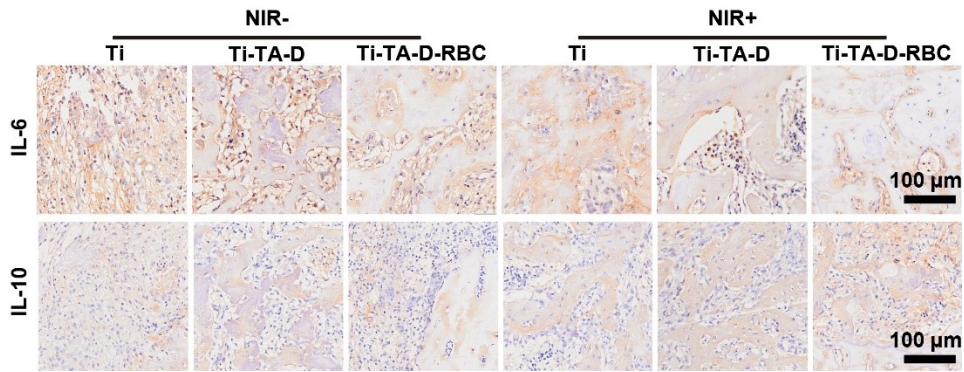


**Fig. S23** Immunohistochemical staining of IL-6 and IL-10 after 1 week of implantation.

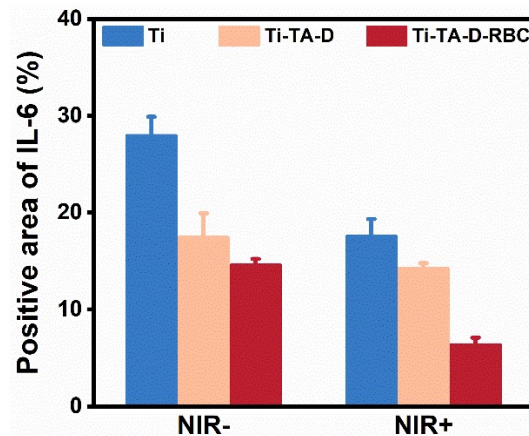


**Fig. S24** The positive area of IL-6 in immunohistochemical staining.

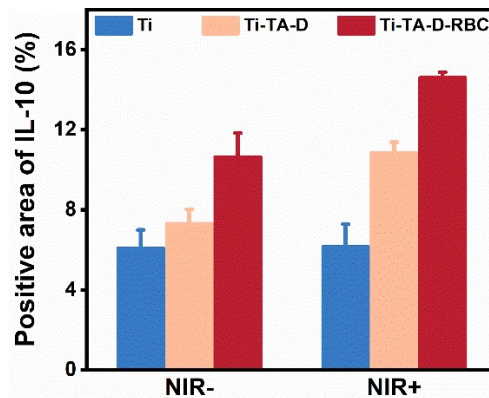


**Fig. S25** The positive area of IL-10 in immunohistochemical staining.

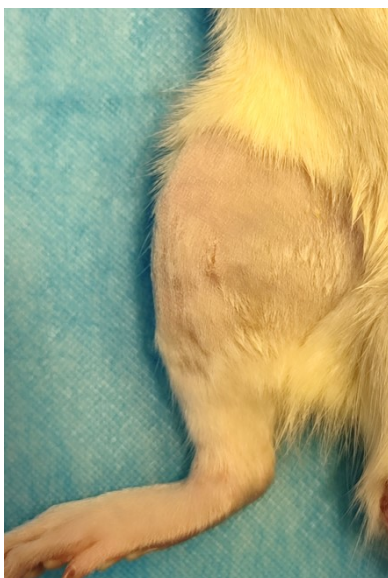


**Fig. S26** Photos of the skin tissues at the implant site in the Ti-TA-D-RBC (NIR+) group.

**Table S2** The comparison of Ti-TA and Ti-TA-D-RBC under NIR irradiation *in vivo*.

group	Temperature under NIR for 10 min	Anti-bacterial ratio	bone volume fraction at 8 weeks
Ti-TA-D	$42.90 \pm 0.26$ °C	$84.05 \pm 0.76\%$	$28.64 \pm 0.94\%$
Ti-TA-D-RBC	$50.57 \pm 0.29$ °C	$99.97 \pm 0.02\%$	$70.70 \pm 1.78\%$
Increasing ratio	1.18 times	1.19 times	2.47 times

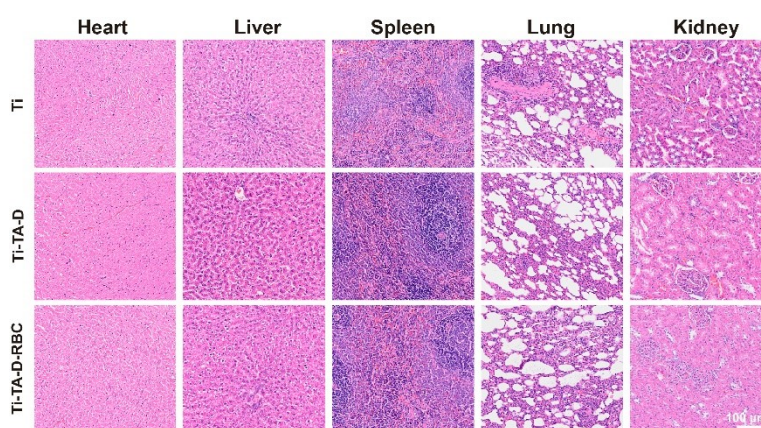


**Fig. S27** H&E staining of major organs (heart, liver, spleen, lung, and kidney) of different groups.

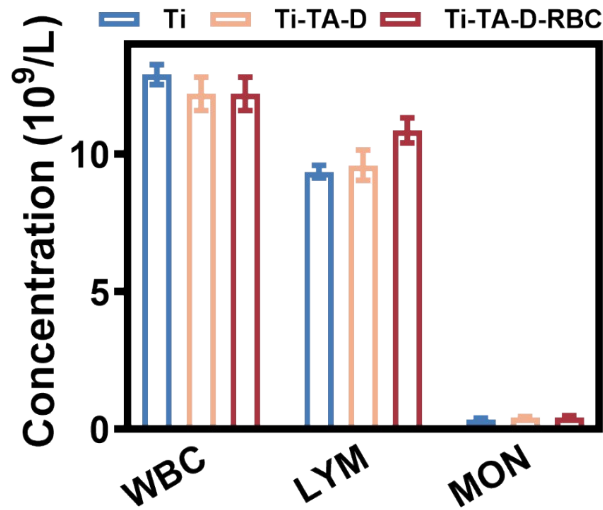


**Fig. S28** Assessment of systemic inflammation by analysis of the white blood cells (WBC), lymphocytes (LYM) and monocytes (MONO) in peripheral blood.

**Table S3** The primer sequence used in this study.

	Primer sequences (5'-3')
IL-10 Forward	ATTTGAATTCCTGGGTGAGAAG
IL-10 Reverse	CACAGGGGAGAAATCGATGACA
TNF- $\alpha$ Forward	TCTTCTCATTCCTGCTTGTGG
TNF- $\alpha$ Reverse	GGTCTGGGCCATAGAACTGA
CD206 Forward	TTGGACGGATAGATGGAGGG
CD206 Reverse	CCAGGCAGTTGAGGAGGTTC
CD86 Forward	TCTGCCGTGCCATTTACAA
CD86 Reverse	TGTGCCCAAATAGTGCTCGT
IL-6 Forward	AACGATGATGCACTTGCAGA
IL-6 Reverse	GAGCATTGGAAATTGGGGTA
IL-1 $\beta$ Forward	CAACCAACAAGTGATATTCTCCATG
IL-1 $\beta$ Reverse	GATCCACACTCTCCAGCTGCA
ALP Forward	CATCATGTTCCTGGGAGATG
ALP Reverse	GGTGTTTGTACGTCTTGGAGA
BMP-2 Forward	CGGTCTCCTAAAGGTCGACCAT
BMP-2 Reverse	CGAACTTCTTGCGGCCAGCT
RUNX2 Forward	CGA CAG TCC CAA CTT CCT GT
RUNX2 Reverse	CGG TAA CCA CAG TCC CAT CT
GAPDH Forward	ACCCAGAAGACTGTGGATGG
GAPDH Reverse	CACATTGGGGGTAGGAACAC

## **MATERIALS AND METHODS**

### **Materials**

Ti implants, including Ti disks ( $1 \times 1 \text{ cm}^2$ , 0.2 mm in thickness) and Ti rods (2 mm diameter, 6 mm length) were purchased from Shengze Metal Ltd (Baoji, China). TA was purchased from Sigma-Aldrich (Shanghai, China). Dex was obtained from Solarbio Biotechnology Ltd (Beijing, China). Alpha modified Eagle's medium ( $\alpha$ -MEM), Dulbecco's modified Eagle's medium (DMEM), fetal bovine serum (FBS), and penicillin–streptomycin solution were obtained from Baoxin Biotechnology Ltd (Chengdu, China). Calcein-AM/PI Live/Dead Cell Double Staining Kit and CCK-8 Assay Kit were obtained from Soleberg Technology Co (Beijing, China). All other chemical agents were procured through the Baoxin Biotechnology Ltd (Chengdu, China), unless a specific alternative source is explicitly indicated.

### **Preparation of the samples**

#### **RBC membrane derivation**

RBC membranes were obtained according to the method reported in a previous article. The whole blood was extracted from Sprague-Dawley rats (8-10 weeks, purchased from Chengdu Dashuo Experimental Animal Co.) Then the harvested whole blood was centrifuged at 3000 rpm for 5 min at  $4^\circ\text{C}$  and washed with PBS solution ( $\text{pH} = 7.4$ ) for three times to obtain RBCs. After washed, the RBCs were cracked in hypotonic solution ( $0.25 \times \text{PBS}$ ) at  $-20^\circ\text{C}$  for 20 min followed by centrifugation at 10000 rpm for 5 min to obtain RBC ghost. Fresh RBC ghost was immediately resuspended in PBS ( $\text{pH} = 7.4$ ) and repeated freeze-thaw to obtain RBC membranes. BCA Protein Assay Kit was used to detect the membrane protein content which was applied to ensure the content of the RBC membrane.

The Ti disks ( $10 \times 10 \text{ mm}$ ) were successively cleaned by acetone, ethanol and ultrapure (UP) water. After air-dried, the clean Ti disks were immersed in TA solution ( $20 \text{ mg mL}^{-1}$ ) in Borate-buffered solution ( $\text{pH} = 9.8$ ) and irradiated under a UV lamp at ( $280 \text{ nm}$ ,  $6 \text{ mW cm}^{-2}$ ) for 4 h to prepare the Ti-TA. Then the Ti-TA was rinsed thoroughly with UP water three times and dried in air. Subsequently  $100 \mu\text{L}$   $5 \text{ mg mL}^{-1}$  Dex solution was dropped onto Ti-TA for 6 h and followed by the same washing and drying steps as

described above to obtain Dex loaded Ti-TA (referred to as Ti-TA-D). Finally, in the stage of fabricating the RBC membrane modified Ti-TA-D (referred to as Ti-TA-D-RBC), the RBC membrane ( $0.2 \text{ mg mL}^{-1}$ ) was sonicated for 5 min (42 kHz, 100 W) to generate a suspension of RBC vesicle. After the sonication, 100  $\mu\text{L}$  RBC vesicle suspension was dropped onto Ti-TA-D for 24 h at ambient room temperature. Similarly, the RBC membrane coating on the PEEK was prepared for thickness measurement using the same method employed for the Ti-TA-D-RBC.

### **Surface characterization**

The surface chemical structures of each group were analyzed using Attenuated total reflectance-Fourier transform infrared (ATR-FTIR) spectra (Nicolet iS10, Thermo Scientific, USA). And further the composition of each layer was detected by X-ray photoelectron spectroscopy (XPS, AXIS Supra, Kratos Analytical, UK). Morphologies and the thickness of RBCM were observed via scanning electron microscope (SEM, Apreo S HiVoc, USA) and Atomic Force Microscopy (AFM, SPM-9600, Shimadzu Corporation, Japan) was also employed to estimate the surface as well as the surface roughness. And for a detailed observation of the RBC membrane's morphology, fresh Ti-TA-D-RBC samples were examined with RSEM (Apreo S/EDX, USA). The hydrophilicity was measured by water contact angle (WCA) using a DSA25 (CA, KRUSS, Germany) using the sessile drop method. 1  $\mu\text{L}$  of water was used as the working fluid. The measurement was repeated in triplicate at different positions and three samples were detected for each group. To assess the morphological stability of Ti-TA-D-RBC, DiO-stained RBC membranes were utilized. The samples were immersed in PBS and flowing water to evaluate their static and dynamic stabilities, respectively. Observations were made using an inverted fluorescence microscope (Leica, Germany) on days 0, 7, 14, 21, and 28, with re-dyeing at selected time points. All the fluorescence intensity in this study was quantified by Image J software. The structural stability of the Ti-TA-D-RBC samples was assessed using ATR-FTIR and XPS, both before and after immersion in PBS for 7 days.

### **Anti-fouling effect evaluation assays**

FITC loaded bovine serum protein (FITC-BSA) were used to evaluate the

antibiofouling properties of the RBC membrane coating. Samples were incubated with 0.1 mg mL<sup>-1</sup> of FITC-BSA at 37 °C for 24 h in darkness. After rinsing with PBS, they were imaged using an inverted fluorescence microscope (Leica, Germany).

### **Photothermal properties evaluation**

High precision thermal infrared thermal imager was employed to capture the thermographic profiles of different samples, followed by an intricate analysis of these thermographic data using the HIKMICRO Analyzer. Ti, Ti-TA, Ti-TA-D, and Ti-TA-D-RBC were exposed to NIR (808 nm, 1.0 W cm<sup>-2</sup>). To elucidate the impact of RBCM on the photothermal conversion efficiency, RBC membrane of different concentration (0.5×, 1×, 1.5×) was used to prepare Ti-TA-D-RBC and similarly exposed to NIR radiation. Throughout the temperature escalation phase, temporal temperature variations were meticulously documented at 30-second intervals over a duration of 10 min. Concurrently, during the temperature descent phase, recordings were made every 5 s for 2 min. Moreover, the photothermal stability of different samples was tested over three heating-cooling cycles of 10 min each. Finally, the thermal diffusivity of different samples was detected by Flash Method Laser Thermal Conductivity Analyzer (LFA 467 HyperFlash, NETZSCH, Germany).

### ***In vitro* Antibacterial Assays**

Both *Staphylococcus aureus* (*S.aureus*) and *Escherichia coli* (*E.coli*) were applied to evaluate antimicrobial effects. Luria-Bertani (LB) broth served as the medium for bacterial cultivation. The bacterial solution was diluted to achieve a concentration at 1.0 × 10<sup>8</sup> CFU mL<sup>-1</sup>. For the samples within the NIR+ group, an exposure to NIR (808 nm, 1.0 W cm<sup>-2</sup>) irradiation was conducted for a duration of 10 min. Immediately following the irradiation, the sample was swiftly submerged into a centrifuge tube containing 5 mL PBS and ultrasound to dilution. Subsequently, 20 μL diluted bacterial solution was evenly spread on LB agar plates and cultured at 37°C overnight. After incubation, digital photos were taken to record the representative images of the culture plates, and the number of colonies on the LB agar plate was counted. The following formula was applied to compute the corresponding relative antibacterial ratio of each group.

$$\text{Antibacterial ratio (\%)} = \frac{A_C - A_E}{A_C} \times 100\%$$

where  $A_C$  is the average CFU of the control group (Ti without NIR irradiation), and  $A_E$  is the average CFU of the other groups. The antibacterial effects were further verified through Live/Dead bacterial staining using the samples treated in the same manner as the spread plate test. The diluted bacterial suspension was transferred to a new 24-well plate and stained for 20 minutes with the LIVE/DEAD BacLight Bacterial Viability Kit (Invitrogen, USA). Observations were made under an inverted fluorescence microscope (Leica, Germany).

The morphologies of *S.aureus* and *E.coli* on different samples were also observed via SEM. The samples were processed identically to in the same manner as the spread plate test. The samples with bacterial on the surfaces were fixed using 2.5% EM-grade glutaraldehyde for 4 h. Continuously, the disks were dehydrated via gradient ethanol solutions (30, 50, 70, 85, 95, and 100% v/v) for 10 min each. Finally, the *S.aureus* and *E.coli* on the different samples were observed by SEM.

#### **Anti-Biofilm Performance in vitro**

The disks of each group were placed in a 24-well plate to which 1 mL *S.aureus* suspension ( $1 \times 10^8$  CFU mL<sup>-1</sup>) was added. The bacteria were cultivated at 37°C for 3 days to obtain biofilms on the disks. The medium was refreshed every 24 h, and the disks were gently washed thrice with aseptic PBS to remove non-adherent bacteria.

The mature biofilms of *S.aureus* were then irradiated/unirradiated by NIR (808 nm, 1.0 W cm<sup>-2</sup>) for 10 min. The antibiofilm capabilities of the different groups were evaluated using Crystal Violet and Live/Dead bacterial staining. For Crystal Violet staining, biofilms post-treatment were fixed with 2.5% v/v glutaraldehyde for 20 minutes, followed by staining with 0.1% Crystal Violet for another 20 minutes. For Live/Dead bacterial staining, the biofilms were washed thrice with sterile PBS and stained for 20 minutes in the dark using the LIVE/DEAD BacLight Bacterial Viability Kit. The red and green fluorescence was observed under a 3D Confocal Laser Scanning Microscope (CLSM, Nikon, Japan).

#### **Cytocompatibility study of each sample**

The rat bone marrow stromal cells (BMSCs) were applied to evaluate the cytotoxicity of as-prepared coatings. The cells were cultured in complete  $\alpha$ -MEM medium supplement with 10% fetal bovine serum and 1% penicillin–streptomycin under a humidified atmosphere of 5% CO<sub>2</sub> at 37°C. The culture medium was replaced every two days. Live/Dead staining was performed to evaluate the cytotoxicity after cultured with the extract solution after 1, 3 and 5 d. The extract solution was obtained by immersing each sample in 1 mL complete  $\alpha$ -MEM medium for 24 h. Live cells were stained with green fluorescence by calcein-AM, the dead cells were stained with red fluorescence with PI, and observed using a fluorescence inverted microscope (Leica, Germany). Besides, the Cell Counting Kit-8 (CCK-8) were carried out to assess cell proliferation. Briefly,  $1 \times 10^4$  cells were seeded in a 96-well plate and cultured for 1, 3 and 5 d. After washed twice with PBS softly, the cells were immersed into the fresh culture medium mixed with 10% CCK-8 solution and co-cultured for 2 h. The absorbance at 450 nm was measured.

### **Cell Morphology**

Cell morphology on various coatings was assessed using fluorescent staining. rBMSCs were fixed with 4% paraformaldehyde after 3 d coculture, then permeabilized with 0.5% Triton X-100 in PBS. Cytoskeletons were stained red with TRITC-phalloidin for 30 minutes at darkroom, followed by nuclei staining with DAPI (blue) for 10 minutes. Post-washing with PBS, images were acquired using a fluorescence inverted microscope (Leica, Germany).

### ***In vitro* anti-inflammation activity assessment**

#### ***In vitro* Dex releasing**

The Dex releasing profiles of Ti-TA-D, Ti-TA-D-RBC, and Ti-TA-D-RBC with NIR irradiation named Ti-TA-D-RBC (+) were investigated. Briefly, each sample was placed in 24-well plates and immersed in 500  $\mu$ L PBS (pH = 7.4). The 24 -well plates were then incubated at 37°C under 150 rpm min<sup>-1</sup>. The Ti-TA-D-RBC (+) group was irradiated with NIR (808 nm, 1.0 W cm<sup>-2</sup>) only for the first 10 min. At predefined intervals, the complete volume of the release medium was taken out and replaced with another same volume of fresh PBS. The release medium was quantitatively analyzed

via high performance liquid chromatography (HPLC) (Agilent, America). Standard calibration curve was obtained by tested the concentration of Dex ranged from 0 to 100  $\mu\text{g mL}^{-1}$ . The mobile phase, methanol/water (70/30 v/v) with a flow rate of 1  $\text{mL min}^{-1}$ , with concentrations ascertained at a wavelength of 240 nm. And 10  $\mu\text{L}$  of release medium was injected for analytical. Three distinct samples of each group were tested for statistical analysis.

#### **Acquisition of extracts of different samples**

The extracts of each group were prepared by immersed sterilized samples with complete DMEM medium. A sample (1  $\text{cm} \times 1 \text{cm}$ ) were immersed in 1 mL medium with sustained shaking at a speed of 150 rpm at 37°C for 24 h on a shaking table. The samples of Ti-TA-D-RBC group were divided into NIR (-) and NIR (+). The NIR (+) group was irritated with 808 nm irradiation for 10 min with the power density of 1  $\text{W cm}^{-2}$  before sustained shaking.

#### ***In vitro* immunomodulation assessment**

Raw 264.7 was chosen to estimate the anti-inflammation activity. Cells were seeded in a 6-well plate at a density of  $5 \times 10^5$  cells per well and incubated overnight, Then to establish an inflammation model, the culture medium was replaced with 10  $\mu\text{g mL}^{-1}$  LPS in complete DMEM medium, which was incubated with different extracts (Ti, Ti-TA, Ti-TA-D, Ti-TA-D-RBC, and Ti-TA-D-RBC+NIR) for 24 h. As a control, untreated Raw 264.7 cells were cultured in complete DMEM medium. After coculture for 24 h, cells and supernatant were collected and analyzed based on immunofluorescence staining, real-time quantitative polymerase chain reaction (RT-qPCR) assay, and enzyme-linked immunosorbent assay (ELISA), respectively.

For immunofluorescence staining (IF), by the end of coculture, cells on the 24-well plate were fixed with 4% paraformaldehyde, permeabilized with 0.25% Triton-X, and blocked with 3% BSA. For the staining of inducible nitric oxide synthase (iNOS), RAW 264.7 of different groups were incubated with anti-iNOS antibody (1:100, Abcam, USA). And donkey anti-rabbit antibody, Alexa Fluor 555 (1:100, Beyotime, China) was selected as secondary antibody. The cell nuclei were stained with DAPI. Images were captured using an invert fluorescence microscope (Leica, Germany).

For RT-qPCR, the cells after coculture were collected using TRIzol reagent (Invitrogen, USA). Total RNA of cell lysates was extracted using a commercial RNA extraction kit (TaKaRa, Japan) and reverse-transcribed into complementary DNA (cDNA) using PrimeScript RT Master Mix (TaKaRa, Japan). RT-qPCR was performed using specific primers and TB Green Premix Ex Taq kit (TaKaRa Bio, Japan) on a RT-qPCR machine (QuantStudio™ 6, Thermo Fisher). The sequences of primer (IL-6, IL-1 $\beta$ , TNF- $\alpha$ , IL-10, CD206, and CD86) are listed in Table S1.

For measurements of cytokine by ELISAs, the supernatants of RAW 264.7 coculture with LPS and extracts for 24 h were collected and inflammatory cytokine (IL-6 and IL-10) were detected by ELISA kits (Meimian, China) following the manufacturer's instructions.

#### ***In vitro* osteogenic effects assessment**

The supernatants of RAW 264.7 stimulated by LPS and different extracts (Ti, Ti-TA, Ti-TA-D, Ti-TA-D-RBC) were collected at 24 h. To prepare the osteogenic-conditioned medium, the supernatants were mixed with the osteogenic differentiation media (complete DMEM medium supplemented with 50  $\mu$ M ascorbic acid, 10 mM  $\beta$ -glycerophosphate, and 0.1  $\mu$ M dexamethasone) at a ratio of 1:5. rBMSCs were seeded in 12-well plates at a density of  $2.5 \times 10^4$  cells per well and the culture medium was replaced by osteogenic-conditioned medium after 24 h coculture. In the following days of incubation, medium was replaced every 3 d.

After 7 days of osteoinduction, ALP staining and quantitative ALP activity were carried out using the BCIP/NBT ALP Color Development Kit (P0321S, Beyotime, China) and Alkaline Phosphatase Assay Kit (C3206, Beyotime, China), respectively. Following 14 days of osteoinduction, ARS staining was performed to evaluate mineral nodule deposits. The cells were stained with ARS (2%, pH4.2, solarbio, China) for 15 min at room temperature after fixed with 4% paraformaldehyde. The results of ALP staining and ARS staining were observed by a stereomicroscope (Olympus SZX16, Japan).

The osteogenic gene expressions of ALP, BMP, and RUNX2 in rBMSCs after osteoinduction for 7 days were detected by RT-qPCR. The amount of corresponding genes expression was normalized to GAPDH and the primer sequences were exhibited

in Table S3.

### **Animal Experiments**

Thirty-six female 8-week-old Sprague-Dawley rats (280-300 g) were bought from the Chengdu Dashuo Experimental Animal Co. All the animal experiments were approved by the Animal Ethics Committee of West China School of Stomatology, Sichuan University. All the animals were randomly divided into three groups (Ti, Ti-TA-D and Ti-TA-D-RBC).

The preparation procedure of Ti-TA-D rods and Ti-TA-D-RBCs mirrored that of disks. After a 7-day acclimatization, the SD rats were anesthetized using an intraperitoneal injection of 2% pentobarbital sodium at a dosage of 40 mg/kg. Then, cylindrical critical-size defects measuring  $\Phi$  2 mm  $\times$  6 mm were surgically created in the tibia of the rats' hind legs using a 2 mm drill. Post-surgery, each defect was in situ injected with  $10^6$  CFU of *S.aureus*. Subsequently, both hind legs of each rat were bilaterally implanted with Ti/Ti-TA-D/ Ti-TA-D-RBC rods (2 mm diameter, 6 mm length) On days 0, 1, 2, and 3 after implantation, the implant sites of the right tibia (NIR+ group) were irradiated with NIR light (808 nm, 1 W cm<sup>-2</sup>) for 10 min each time. One-week post-implantation, 4 rats from each group were euthanized to evaluate the antibacterial efficiency and immunomodulatory properties. The remaining 8 rats of each group were sacrificed at 4 weeks and 8 weeks post-implantation to assess osteogenesis. At the 8-week sacrifice point, main organs including the heart, liver, spleen, lung, and kidney, as well as whole blood, were collected for further testing.

In the *in vivo* antibacterial assessment, the rods were rolled on a LB agar plate for one round, and then cultured for 24 h at 37°C. Post rolling, the rods were placed in round-bottom polystyrene tubes containing 5 mL LB culture and incubated for 6 hours at 37°C. Additionally, exudate from around the implantation site was collected, diluted, and spread onto LB agar plates. Meanwhile H&E and Giemsa staining were used to determine the bacterial contamination of soft tissue around the bone implants and bone-tissue. Besides, two inflammatory factors, IL-6 and IL-10, were detected by immunohistochemistry staining (IHC) to assess the *in vivo* immune modulating properties. All the sections in this study were scanned by research grade all glass

scanning system VS200 (Olympus, Japan).

To evaluate osteogenesis effect, the tibias with different samples were harvested and scanned by microcomputed tomography system (micro-CT) (Skyscan 1275, Bruker, Germany) to evaluate the newly formed bone. The micro-CT operated at 90 kV, 88 mA with a 100 ms exposure time. Three-dimensional (3D) images were reconstructed and analyzed by Mimics Research software. Quantitative analysis of new bone was done by measuring trabecular bone volume fraction (BV/TV), thickness (Tb.Th), number (Tb.N), and separation (Tb.Sp) using CTAn software. Additionally, corresponding sections were stained with hematoxylin and eosin (H&E), Masson's trichrome, and immunohistochemical (IHC) staining for further examination.

### **Statistical Analysis**

Statistical analysis of the results was performed using Origin2019 and GraphPad Prism 9 software. One-way analysis of variance (ANOVA) was used to evaluate differences between groups. Data are expressed as mean  $\pm$  standard deviation ( $n \geq 3$ ). The levels of statistical significance are denoted as follows: \* $p < 0.05$ , \*\* $p < 0.01$ , and \*\*\* $p < 0.001$ , \*\*\*\* $p < 0.001$ .